Great Plains Drought in Simulations of the Twentieth Century

RACHEL R. MCCRARY AND DAVID A. RANDALL

Colorado State University, Fort Collins, Colorado

(Manuscript received 29 January 2009, in final form 14 October 2009)

ABSTRACT

Coupled global circulation models (CGCMs) have been widely used to explore potential future climate change. Before these climate projections can be trusted, the ability of the models to simulate present-day climate must be assessed. This study evaluates the ability of three CGCMs that participated in the Fourth Assessment Report of the Intergovernmental Panel on Climate Change to simulate long-term drought over the Great Plains region with the same frequency and intensity as was observed during the twentieth century. The three models evaluated in this study are the Geophysical Fluid Dynamics Laboratory Coupled Model, version 2.0 (CM2.0); the National Centers for Atmospheric Research Community Climate System Model, version 3 (CCSM3); and third climate configuration of the Met Office Unified Model (HadCM3).

The models are shown to capture the broad features of the climatology of the Great Plains, with maximum precipitation occurring in early summer, as observed. However, all of the models overestimate annual precipitation rates. Also, in CCSM3, precipitation and evapotranspiration experience unrealistic decreases between the months of June and August.

Long-term droughts are found in each simulation of the twentieth century that are comparable in duration, severity, and spatial extent as has been observed. However, the processes found to be associated with simulated long-term droughts vary among the models. In both CM2.0 and HadCM3, low-frequency variations in Great Plains precipitation are found to correspond with low-frequency variations in tropical Pacific SSTs. In CCSM3, on the other hand, there appears to be no significant correlation between tropical Pacific SST variability and Great Plains precipitation. Strong land–atmosphere coupling in CCSM3 may explain the persistence of long-term droughts in this model.

1. Introduction

The risk of future long-term drought (a dry period that exhibits below-average annual precipitation for 5 yr or longer) is one of the biggest concerns facing the Great Plains region of the United States (defined here as the region bounded by 30°–50°N, 95°–105°W). Droughts have serious social, economic, and environmental consequences and can negatively impact surface and groundwater supplies, water quality, agriculture and rangeland productivity, natural ecosystems, and recreation (Kallis 2008). The Great Plains region is expected to become increasingly vulnerable to drought as the demand for water increases because of enhanced agricultural production and growing populations, and water continues to be pumped unsustainably from the Ogallala Aquifer (Jacobs et al. 2000). Reminders of the devastating Dust Bowl drought of the 1930s and the Southwest drought of the 1950s lead water managers to ask how future climate change may influence precipitation over the Great Plains region.

Coupled global circulation models (CGCMs) are often employed to help make future climate change projections. A recent study by Seager et al. (2007) uses the CGCMs that participated in the Fourth Assessment Report (AR4) of the Intergovernmental Panel on Climate Change (IPCC) to show that the southwestern United States, including portions of the Great Plains, may become increasingly arid in the future. Although CGCMs are important tools for understanding possible future climate change, our limited understanding of the complex climate system and the factors that influence precipitation variability makes assessing the accuracy of the CGCMs projections a challenge.

One way to evaluate the performance of CGCMs is to compare their simulations of the variations in

Corresponding author address: Rachel McCrary, Department of Atmospheric Science, 1371 Campus Delivery, Colorado State University, Fort Collins, CO 80523.
E-mail: rachel@atmos.colostate.edu

DOI: 10.1175/2009JCLI3061.1

twentieth-century climate with observations. The ability of the models to realistically simulate the observed climate is one measure of their capability to project the future. In this context, we evaluate the ability of three of the AR4 CGCMs to simulate long-term Great Plains drought with the same frequency and intensity as was observed during the twentieth century. The three CGCMs chosen are the Geophysical Fluid Dynamics Laboratory (GFDL) Climate Model, version 2.0 (CM2.0); the National Center for Atmospheric Research (NCAR) Community Climate System Model, version 3.0 (CCSM3); and third climate configuration of the Met Office (UKMO) Unified Model (HadCM3).

To successfully simulate long-term drought, the models must not only capture the observed low-frequency variability in Great Plains precipitation, but they must also accurately represent the processes that cause and maintain the droughts. Although considerable effort has been expended to understand the causes of long-term Great Plains drought, the processes involved have not yet been fully established. Observational and modeling studies alike point to several variations of the climate system that are correlated with drought conditions over the Great Plains (Borchert 1950; Namias 1960; Borchert 1971; Namias 1983; Oglesby 1991; Ting and Wang 1997; Ropelewski and Halpert 1986; Trenberth and Branstator 1992; Livezey and Smith 1999). These include but are not limited to the following: variations in sea surface temperature (SST) patterns in the North Pacific, North Atlantic, Indian Ocean, tropical Atlantic, and tropical Pacific; changes in storm tracks; and changes in the strength and position of the Bermuda high. Studies also indicate that land–atmosphere feedbacks play an important role in the initiation and persistence of long-term droughts over the Great Plains region (Namias 1991; Oglesby and Erickson 1989; Schubert et al. 2004a, 2008).

Although these factors may all contribute to dryness over the Great Plains in some ways, for reasons discussed later it appears that three primary mechanisms cause Great Plains precipitation anomalies to persist for long periods of time. These are 1) variations in tropical Pacific SSTs, 2) variations in tropical North Atlantic SSTs, and 3) land–atmosphere interactions that involve feedbacks between soil moisture and rainfall.

Recently, modeling studies that use atmospheric global circulation models (AGCMs) forced with historic time series of global SSTs have implicated cool, La Niña–like conditions in the tropical Pacific as the primary cause of long-term Great Plains drought (Schubert et al. 2004a,b; Seager et al. 2005a,b, 2007; Cook et al. 2007; Seager et al. 2008). Similar modeling studies have also shown that three long-term droughts that occurred in the mid-to-late nineteenth century were also forced by variations tropical Pacific SSTs (Herweijer et al. 2006). These studies point to a number of different ways in which tropical Pacific SSTs are linked to changes in North American precipitation. For example, Seager et al. (2005a) found that changes in tropical Pacific SSTs are associated with changes in the subtropical jets, which affect the propagation of transient eddies, leading to changes in the eddy-driven mean meridional circulation (MMC). When colder than normal conditions are present in the tropical Pacific, changes in the MMC can result in enhanced subsidence over the Great Plains, thereby triggering drought.

Observational and modeling studies have also suggested that low-frequency variations in tropical North Atlantic SSTs may modulate Great Plains precipitation variability on decadal time scales (Schubert et al. 2004b; Sutton and Hodson 2005, 2007; McCabe et al. 2008). The extent to which tropical Atlantic SSTs influence Great Plains drought appears to vary from case to case, but studies show that during both the 1930s and 1950s droughts, which were notably the most severe, long-lasting droughts of the twentieth century, warmer than normal conditions persisted in the tropical North Atlantic (from the equator to 30°N). The exact mechanism by which tropical North Atlantic SST variations may influence Great Plains precipitation is not fully known; it is possible that warmer than normal SSTs in this region impact the position and strength of the Bermuda high and restrict the flow of moisture into the Great Plains region (Woodhouse and Overpeck 1998).

Land–atmosphere interactions and feedbacks between soil moisture and rainfall may also to contribute to drought conditions over the Great Plains. Studies that highlight the importance of soil moisture conditions in the generation and perpetuation of precipitation anomalies include those of Namias (1991), Findell and Eltahir (1997), Eltahir (1998), Schubert et al. (2004a), Pal and Eltahir (2001), Koster et al. (2003, 2004, 2006), and Guo et al. (2006). Land–atmosphere interactions influence Great Plains precipitation by regulating evapotranspiration from surface (i.e., precipitation recycling). In addition, soil moisture can impact precipitation indirectly by affecting boundary layer characteristics and atmospheric stability. Some studies suggest that soil moisture rainfall feedbacks may act as a bridging mechanism between cool-season precipitation anomalies, which result from SST forcing, and warm-season precipitation anomalies (Seager et al. 2005b; Cook et al. 2007). Koster et al. (2000) and Schubert et al. (2008) argue that, in the Great Plains region, precipitation is particularly sensitive to changes in soil moisture conditions, especially during the warm months.

The present study addresses the following questions: 1) How well do the three CGCMs simulate the climatology of the hydrologic cycle of the Great Plains? 2) Do

TABLE 1. Coupled global climate models analyzed in this study.

Model	Atmosphere resolution (lat × lon)	No. of levels	Ocean resolution (lat × lon)	No. of soil layers	No. of Simulations	Reference
CM2.0 GFDL	2.0° × 2.5°	24	1° × 1° (0.3°)	10	3	Delworth et al. (2006)
NCAR CCSM3	T85 (1.4° × 1.4°)	26	1.1° × 1.1°	10	8	Collins et al. (2006)
UKMO HadCM3	2.75° × 3.25°	24	1.25° × 1.25°	4	3	Gordon et al. (2000)

the CGCMs simulate long-term Great Plains droughts with the same frequency and intensity as was observed during the twentieth century? 3) What mechanisms influence the simulated long-term droughts, and are they the same as observed?

One of the major challenges for this study is that observational records of precipitation are relatively short (~100 yr in duration) and only a limited number of droughts occurred during the twentieth century. Because long-term droughts have significant societal consequences, studies like this are necessary, but we should keep in mind that we are comparing the models against a limited number of observations.

The structure of this paper is as follows: Section 2 describes the models and datasets used in this study. In section 3, the simulated climatology of the hydrologic cycle of the Great Plains from each model is compared against observations. Section 4 examines the ability of the models to realistically represent the frequency and variability of long-term Great Plains drought. In section 5, the influence of tropical Pacific SST variability, tropical North Atlantic SST variability, and land–atmosphere interactions on the simulated droughts are investigated.

2. Data and methodology

a. Models

As mentioned in section 1, this study utilizes the ''Climate of the 20th Century'' integrations performed with CM2.0, CCSM3, and HadCM3, which were used in the AR4 (Solomon 2007). These simulations were obtained from the World Climate Research Programme (WCRP) Coupled Model Intercomparison Project Phase 3 (CMIP3; Meehl et al. 2007) multimodel dataset (available online at http://www-pcmdi.llnl.gov). Table 1 summarizes some basic properties of the models used in this study.

The twentieth-century climate simulations produced for the AR4 were initialized from preindustrial control runs in which the atmospheric content of trace gases and solar irradiance were representative of the late nineteenth century (Meehl et al. 2007). The simulations also made use of historical time series of observed twentieth-century atmospheric greenhouse gas concentrations, sulfate aerosol direct effects, and volcanic and solar forcings. Multiple integrations of twentieth-century climate were performed with each of the three models and differ only in their initial conditions as determined by the preindustrial control run of each model (Table 1).

b. Datasets

The datasets used to evaluate the CGCM simulations come from many different sources. Descriptions of the datasets can be found in Table 2.

Simulated precipitation is compared with the observational-based dataset the Climate Research Unit Time Series 2.1 (CRU TS 2.1; Mitchell and Jones 2005) from the University of East Anglia. CRU TS 2.1 is a gridded dataset that covers the global land surface at 0.5° × 0.5° resolution for the period 1901–2002 and was developed from station data.

Downwelling shortwave radiation is compared with data from the National Centers for Environmental Prediction (NCEP)–NCAR reanalysis project (called the NCEP reanalysis) obtained from the National Oceanic and Atmospheric Administration (NOAA)/Climate Diagnostics Center (CDC) Web site (available online at http://www.cdc.noaa.gov/cdc/reanalysis/reanalysis.shtml; Kalnay et al. 1996). The NCEP reanalysis extends from January 1948 to the present and has global coverage with at 2.5° × 2.5° resolution and 17 vertical levels. Downwelling shortwave radiation is a class C variable and is therefore completely model derived. It is used here as a comparison with the CGCMs.

For SST data analysis, we use the UKMO Hadley Centre Sea Ice and SST dataset (HadISST; Rayner et al. 2003). HadISST has a 1° × 1° resolution and spans from 1870 to the present.

Observations of hydrologic variables such as soil moisture and evapotranspiration are scarce. It is particularly difficult to find long-term data records (i.e., records longer than a few decades) for these variables over the Great Plains region (Robock et al. 2000). Without observations, it is not possible to make direct estimates of the relationships between precipitation, evapotranspiration, and soil moisture over the Great Plains region. This study utilizes output from a hydrologic modeling study performed by Andreadis et al. (2005, hereafter AEA) to compare with the CGCM data. The AEA study simulated historical soil moisture, evapotranspiration, and

TABLE 2. Observational datasets used to evaluate the CGCMs in this study.

	CRU TS 2.1	VIC	NCEP	HadISST
Origin	Station data	Hydrologic model forced with observed precipitation and surface meteorology	Observations and model forecasts	Observations
Resolution (lat × lon)	0.5° × 0.5°	0.5° × 0.5°	2.5° × 2.5°	1° × 1°
Domain	Global land surface (except Antarctica)	Land surface of continuous United States	Global	Global ocean surface
Variables	Precipitation	Evapotranspiration, soil moisture	Shortwave forcing	SST
Source	Mitchell and Jones (2005)	AEA	Kalnay et al. (1996)	Rayner et al. (2003)

runoff over the contiguous United States for the period 1920–2003 at 0.5° × 0.5° spatial resolution using the variable infiltration capacity (VIC) macroscopic hydrologic model (Liang et al. 1994, 1996; Cherkauer and Lettenmaier 2003). AEA accomplishes this by forcing the VIC model with observed precipitation and near-surface meteorology for the twentieth century to estimate soil moisture, runoff, and evapotranspiration rates. Results from the AEA study will be used as a proxy for direct observations. Because these data are model derived, they should be treated with caution throughout the text.

c. Methodology

This study defines the Great Plains of the United States as the area that lies between 30° and 50°N and between 95° and 105°W. This is the same as the definition used by Schubert et al. (2004a). All time series analyses in this study are based on area-weighted averages within this domain. In section 3, the seasonal cycles of hydrologic variables are compared between the models and observations. The climatological values used in this section are computed from the entire time periods of the modeled and observational records. In sections 4 and 5, anomalies of precipitation, SSTs, evapotranspiration, and soil moisture are examined. Anomalies are calculated relative to the seasonal averages computed from the entire time record.

To investigate low-frequency variations in precipitation and SSTs, a low-pass filter is applied to the datasets. This filter retains variability that exists on time scales of 6 yr and longer and was developed by Zhang et al. (1997). The low-pass filter has also been used in previous studies that investigate long-term Great Plains drought (Schubert et al. 2004a,b).

In section 5, indices for tropical Pacific and tropical North Atlantic SST variability are used. We define an index for low-frequency SST variations in the tropical Pacific by averaging the low-pass-filtered SST anomalies over the Niño-3.4 region (5°S–5°N, 120°–170°W). An index for low-frequency variations in tropical North Atlantic SST variability is similarly defined by averaging low-pass-filtered SSTs over all Atlantic Ocean points between the equator and 30°N (the same region defined by Seager et al. 2008).

3. Climatology of the hydrologic cycle of the Great Plains

The first step in assessing the usefulness of the models is to investigate how well they simulate the observed climatology of the Great Plains hydrologic cycle. If the models do not accurately capture the annual cycles of variables such as precipitation and evaporation, their usefulness in studies that require an investigation of the variability about the seasonal mean is questionable. A discussion of the ability of some of the AR4 models to represent the climatology of Great Plains precipitation can be found in Ruiz-Barradas and Nigam (2006).

Figure 1 compares the climatology of the hydrologic cycle of the Great Plains between the observations and the models using time series plots of the composite annual cycles of precipitation, evapotranspiration, and soil moisture. The observed annual cycle of Great Plains precipitation shows marked seasonality, with minimum precipitation in January and maximum precipitation in June (Fig. 1). The observed time series also exhibits a slightly bimodal pattern, with a second weaker maximum in precipitation in September (2.1 mm day^{-1}). Total annual precipitation for the Great Plains region averages 1.54 mm day^{-1}, with the range of the seasonal cycle reaching approximately 2.1 mm day^{-1} (Table 3). It therefore appears that the annual cycle of Great Plains precipitation can be divided into two distinct seasons: a wet season that extends from April to September and a dry season that extends from October to March.

In the models, the annual cycle of Great Plains precipitation also shows large seasonal variations, with minimum precipitation in winter and maximum precipitation in early summer (Fig. 1). All three models tend to overestimate precipitation rates between November and March, possibly because of poor a representation of the surface topography, which reduces the rainshadow effect of the Rocky Mountains. Both CM2.0 and HadCM3

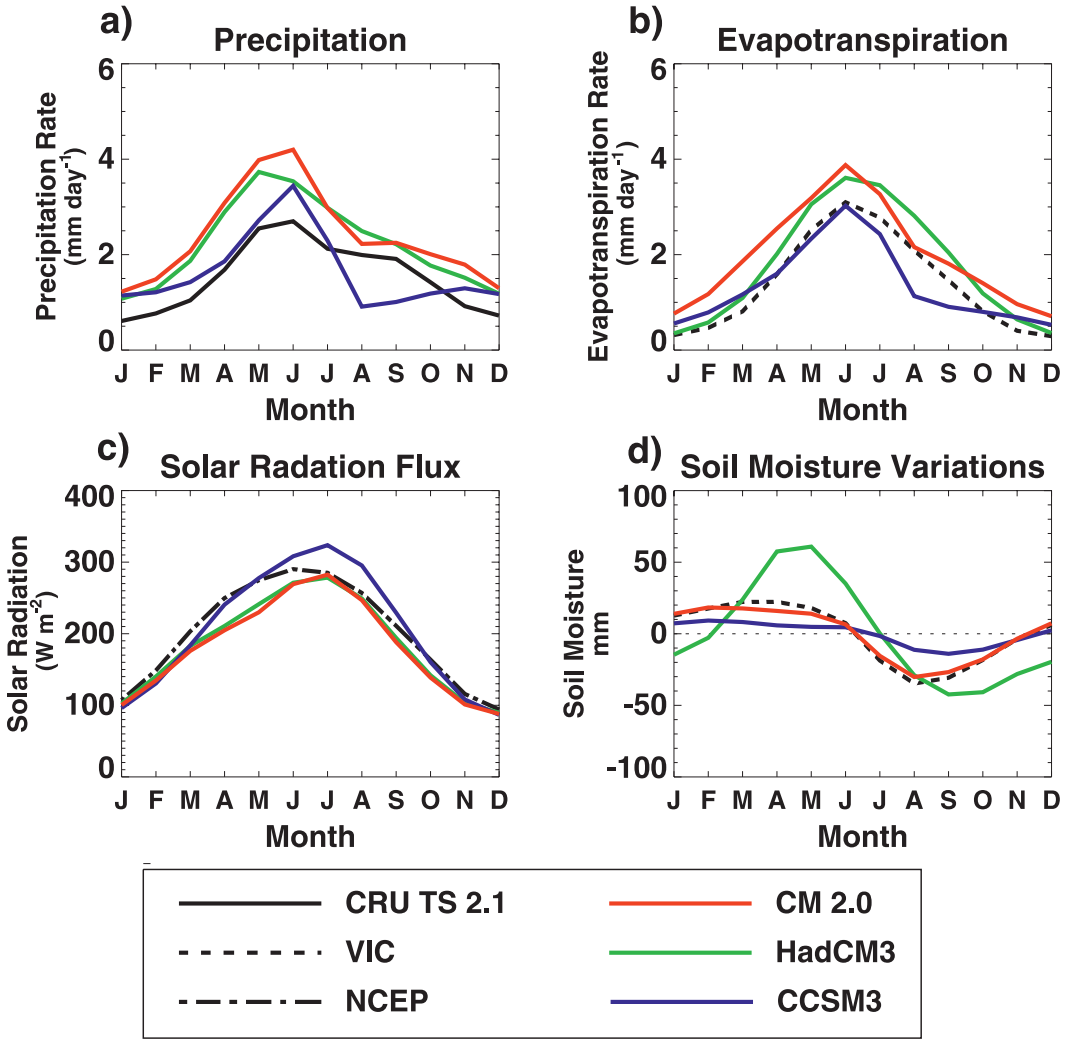

FIG. 1. Time series plots for (a) the annual cycle of Great Plains precipitation (mm day^{-1}), (b) evapotranspiration (mm day^{-1}), (c) shortwave radiation flux (W m^{-2}), and (d) seasonal variations of total column soil moisture (mm) from the various observational sources (black) and the three models [CM2.0 (red), CCSM3 (blue), and HadCM3 (green)].

also overestimate precipitation rates throughout the remainder of the seasonal cycle; maximum precipitation in CM2.0 is almost twice that observed. CCSM3, on the other hand, has difficulty capturing the timing of the seasonal cycle of Great Plains precipitation. In late summer, CCSM3 experiences what could be considered a seasonal drought, in which precipitation drops dramatically between June and August to rates that are below 1 mm day^{-1}. Of the three models, only CM2.0 captures the secondary maximum in precipitation that occurs in September, although the drop in precipitation that occurs between June and August in CM2.0 is much more dramatic than observed. All of the models overestimate mean annual precipitation rates for the Great Plains region, as well as the total range of the seasonal cycle (Table 3).

Much like precipitation, the annual cycle of evapotranspiration averaged over the Great Plains region experiences large seasonal variations (Fig. 1b). Minimum evapotranspiration rates occur in fall and winter when both water and energy availability (measured here as the shortwave radiative flux) at the surface are limited (Figs. 1a,c). Evapotranspiration rates then increase in spring and summer when both water and energy at the surface increase. Throughout the entire seasonal cycle, both CM2.0 and HadCM3 overestimate evapotranspiration rates, compared to VIC. The seasonal drought in precipitation that is seen in CCSM3 in the late summer can be found in the evapotranspiration time series as well. Again, reductions in the amount of water at the surface may account for these reductions in evapotranspiration.

TABLE 3. Values for the mean and the range of the time series of the annual cycle of precipitation, evapotranspiration, and soil moisture averaged over the Great Plains region for the observations and models, as shown in Fig. 1.

	Precipitation (mm day^{-1})		Evapotranspiration (mm day^{-1})		Soil moisture (mm)	
Dataset	Annual mean	Range	Annual mean	Range	Annual mean	Range
Observations	1.54	2.09	1.39	2.81	258.5	57.01
CM2.0	2.38	2.98	1.98	3.17	66.76	48.55
CCSM3	1.62	2.53	1.33	2.50	584.8	23.29
HadCM3	2.21	2.66	1.77	3.26	780.8	103.3

Mean annual climatological total column soil moisture content is shown in Table 3. Total column soil moisture content varies quite dramatically among the CGCMs and VIC. For example, average soil moisture content in HadCM3 is more than three times that observed, whereas total column soil moisture content in CM2.0 is only one quarter of what is found from VIC. These variations may be due to differences in the total depth of the soil column and the water holding capacity of the soils in each model. Figure 1d shows the annual cycle of Great Plains soil moisture content. The mean annual climatological values from Table 3 have been removed so that the timing of the seasonal cycle and the magnitude of the seasonal variations in soil moisture can be more easily compared.

Seasonal variations in total column soil moisture are determined by the seasonal differences between precipitation and evapotranspiration at the surface. In all of the models, soil moisture content increases from late fall to early spring, when precipitation exceeds evapotranspiration (Fig. 1d). During the summer, soil moisture content decreases when evapotranspiration exceeds precipitation. The range of the seasonal cycle of soil moisture is largest in HadCM3, for which soil moisture content varies between spring and fall by 103 mm. The range is smallest in CCSM3, for which soil moisture content varies by only 23 mm. The ranges of the seasonal cycle of soil moisture are comparable between the VIC and CM2.0. Large differences in soil moisture between the models may not be physically based but rather a product of how subsurface processes are parameterized.

In general, the three models capture the broad features of the hydrologic cycle of the Great Plains, but each model exhibits some difficulty in representing the timing and magnitude of the seasonal variations in precipitation, evapotranspiration, and soil moisture. In the next section, the ability of the CGCMs to represent long-term drought is evaluated.

4. Long-term drought

Time series plots of annual-mean Great Plains precipitation anomalies for the observations and one integration from each of the models are shown in Fig. 2 (because of space constraints, we cannot show the time series plots from all of the model integrations, but they can be found in McCrary 2008). These figures demonstrate that precipitation over the Great Plains region is highly variable, even in the annual-mean time series. Great Plains precipitation tends to be more variable in the models than in the observations, as seen by the standard deviation values given in Table 4. This is especially true for CM2.0, for which standard deviation values are almost two-thirds larger than observed.

Because precipitation exhibits so much year-to-year variability, a low-pass filter is applied to the Great Plains precipitation time series to help identify the low-frequency variations that occur throughout the time record. The low-pass-filtered precipitation time series is superimposed on the annual-mean precipitation time series in Fig. 2 (thick black curve). Long-term drought periods are then defined as any period of time where the filtered time series exhibits lower than average precipitation for five years or longer. It is further required that peak anomalies during the drought period exceed one standard deviation away from the mean.

The long-term drought periods found in each time series are highlighted in Fig. 2. These drought periods and the long-term droughts found in the simulations not shown in Fig. 2 are summarized in Table 5. These are fully coupled GCM integrations that are forced only by time series of observed greenhouse gas concentrations, sulfate aerosols, and volcanic eruptions. This implies that, for each model integration, not only are the atmospheric conditions unique, but so are the ocean and land surface conditions. Therefore, it is not expected that the timing of any long-term droughts in the models will coincide with the observed timing. Also, it is expected that the timing of the long-term droughts in each individual model integration (from the same model) will be different. That being said, what we want to see is if the characteristics of Great Plains droughts in the models are similar to those observed. In the following discussion, the frequency of long-term drought depends somewhat on our chosen definition. Similar results have been found by using the

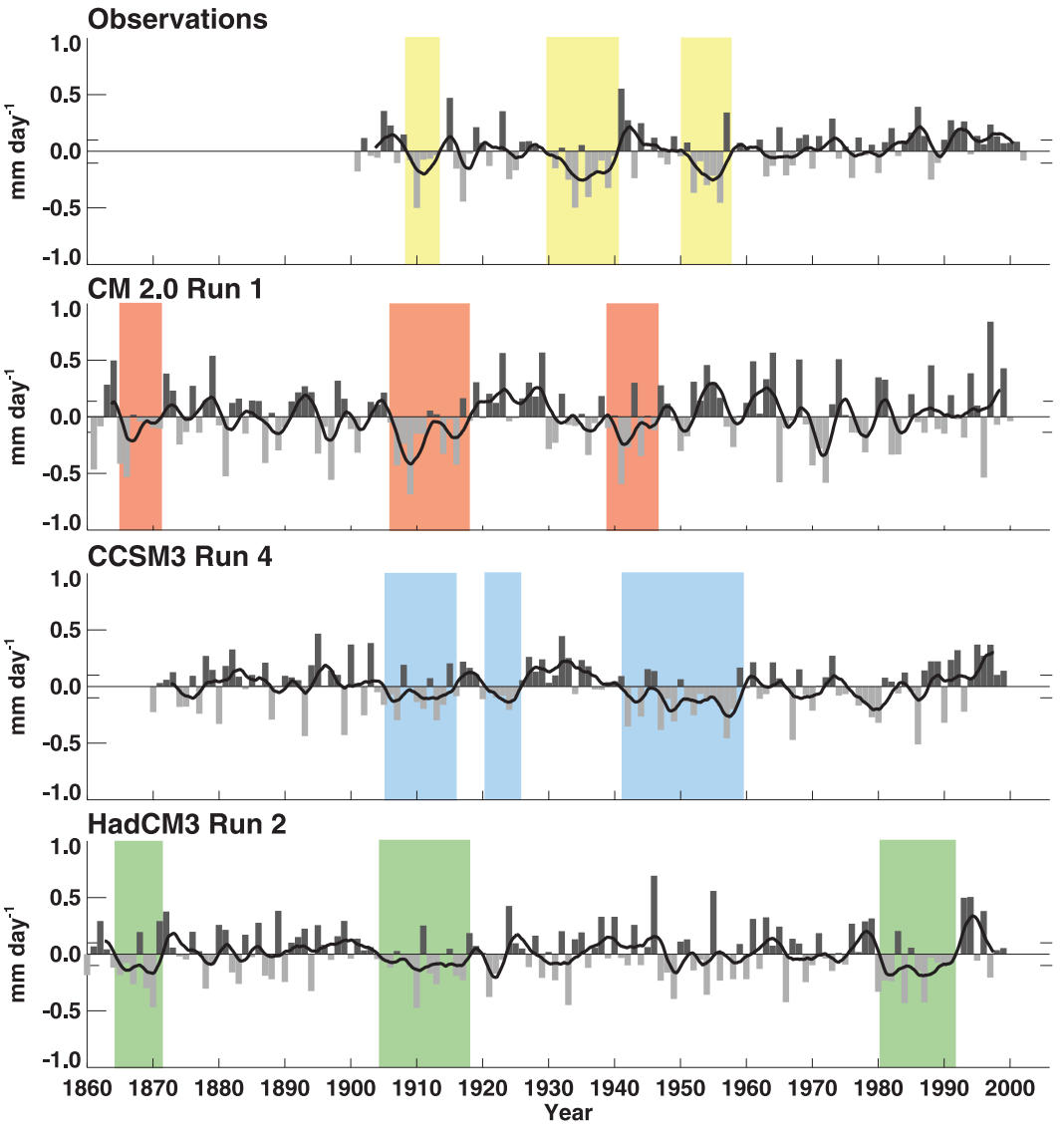

FIG. 2. Time series of annual-mean Great Plains precipitation anomalies (mm day^{-1}) from (a) the observations and one integration from each model: (b) CM2.0 run 1, (c) CCSM3 run 4, (d) HadCM3 run 2. Superimposed on each time series plot is the low-pass-filtered Great Plains precipitation time series (thick black curve). Long-term drought periods are highlighted in each time series. Time series plots from the other model integrations can be found in McCrary (2008).

Standardized Precipitation Index (SPI; McKee et al. 1993) averaged over a 24-month period as an index of long-term drought (not shown).

Three long-term droughts stand out in the observed precipitation time series. The first and weakest drought occurred around 1910. During this period, negative precipitation anomalies primarily influenced the Great Plains region of the United States, where rainfall reductions were largest over southeastern Texas and Oklahoma (Fig. 3a). The second drought spanned the 1930s. This drought is commonly referred to as the Dust Bowl, because it was accompanied by severe dust storms. Although precipitation reductions covered most of the United States during this time period, the central and northern parts of the Great Plains were most heavily impacted (Fig. 3b). The third and final long-term drought of the twentieth century occurred during the 1950s. This drought had a larger impact on the southern Great Plains than either of the two previous droughts (Fig. 3c).

In each simulation of twentieth-century climate, the Great Plains region experienced at least one long-term drought period, with most integrations having up to three or four long-term droughts (Table 5). Table 5 shows that the simulated long-term droughts lasted from

TABLE 4. The std dev of the observed and simulated time series of annual-mean Great Plains precipitation anomalies.

Dataset		Std dev (mm day^{-1})
Observations		0.204
CM2.0	Run 1	0.288
	Run 2	0.296
	Run 3	0.260
CCSM3	Run 1	0.216
	Run 2	0.204
	Run 3	0.217
	Run 4	0.207
	Run 5	0.216
	Run 6	0.208
	Run 7	0.220
	Run 9	0.239
HadCM3	Run 1	0.224
	Run 2	0.230

5 to 20 yr, with most persisting for 7–11 yr. This range is similar to that seen during the real twentieth century. Because the model integrations span over a longer time period than the observational record, Fig. 4 shows the number of long-term droughts that occurred per century from each realization of the twentieth century. From the figure, it appears that the models do capture the observed frequency of long-term droughts. Unfortunately, we are comparing against a small observational sample size, so it is difficult to determine with any statistical measure of confidence if these results are robust. However, we can perform a simple thought experiment to determine theoretical upper and lower bounds for the potential number of droughts that could occur in a 100-yr time record. For the upper bound, by basic probability we know that, at most, five 10-yr-long droughts or ten 5-yr-long droughts could occur in a 100-yr time period. We can then use paleoclimate data to determine the lower bound. Using evidence of drought conditions based on historical documents and proxi-climate data (tree rings, archaeological remains, lake sediments, and geomorphic data), Woodhouse and Overpeck (1998) have estimated that, over the past 400 yr, at least one or two long-term droughts have occurred over the Great Plains per century. This indicates that we can expect at least one long-term drought to occur in the model simulations of the twentieth-century climate. Based on this simple test, it is reasonable to expect that 1–6 long-term droughts could have occurred in the twentieth century. The models clearly fall within this range, so it is reasonable to say that the models do capture the observed frequency of long-term drought.

The spatial patterns of the simulated long-term droughts are shown in Figs. 3d–l. In general, the simulated droughts exhibit spatial patterns similar to those observed during the twentieth century. In many of the simulated droughts, the southern half of the Great Plains region is more heavily impacted than the northern half, as in the observed 1950s drought (Figs. 3e,f,j). In some cases, simulated Great Plains drought extends over most of North

TABLE 5. Summary of the long-term droughts from the observations and the simulations of the climate of the twentieth century. Table includes the total number of droughts in each realization of the twentieth century, the total length of each drought, the years spanned by each drought, and the average precipitation anomalies associated with each drought.

Dataset		No. of droughts	Length of drought (yr)	Drought years	Avg anomaly (mm day^{-1})
Observations		3	5	1908–13	−0.125
			10	1930–40	−0.191
			7	1950–57	−0.149
CM2.0	Run 1	3	6	1865–71	−0.100
			12	1906–18	−0.183
			7	1939–46	−0.116
CM2.0	Run 2	4	9	1924–33	−0.137
			10	1941–51	−0.125
			6	1962–68	−0.154
			6	1986–92	−0.145
CM2.0	Run 3	1	21	1923–44	−0.151
CCSM3	Run 1	4	8	1882–90	−0.177
			9	1929–38	−0.121
			6	1941–47	−0.124
			6	1991–97	−0.109
CCSM3	Run 2	3	7	1892–99	−0.120
			9	1907–16	−0.116
			7	1958–65	−0.085
CCSM3	Run 3	4	8	1950–58	−0.148
			10	1961–71	−0.074
			6	1973–79	−0.074
			6	1991–97	−0.140
CCSM3	Run 4	4	10	1905–15	−0.079
			5	1920–25	−0.084
			19	1940–59	−0.124
			7	1975–82	−0.117
CCSM3	Run 5	3	12	1889–1901	−0.121
			11	1921–32	−0.131
			11	1979–90	−0.085
CCSM3	Run 6	3	7	1886–93	−0.102
			20	1901–21	−0.066
			10	1947–57	−0.093
CCSM3	Run 7	4	8	1876–84	−0.178
			12	1925–37	−0.077
			5	1958–63	−0.082
			9	1988–97	−0.185
CCSM3	Run 9	4	12	1876–88	−0.104
			9	1894–1903	−0.129
			10	1905–15	−0.074
			10	1923–33	−0.123
HadCM3	Run 1	4	10	1869–79	−0.076
			11	1927–38	−0.086
			5	1947–52	−0.103
			16	1974–90	−0.113
HadCM3	Run 2	3	7	1864–71	−0.114
			14	1904–18	−0.083
			11	1980–91	−0.131

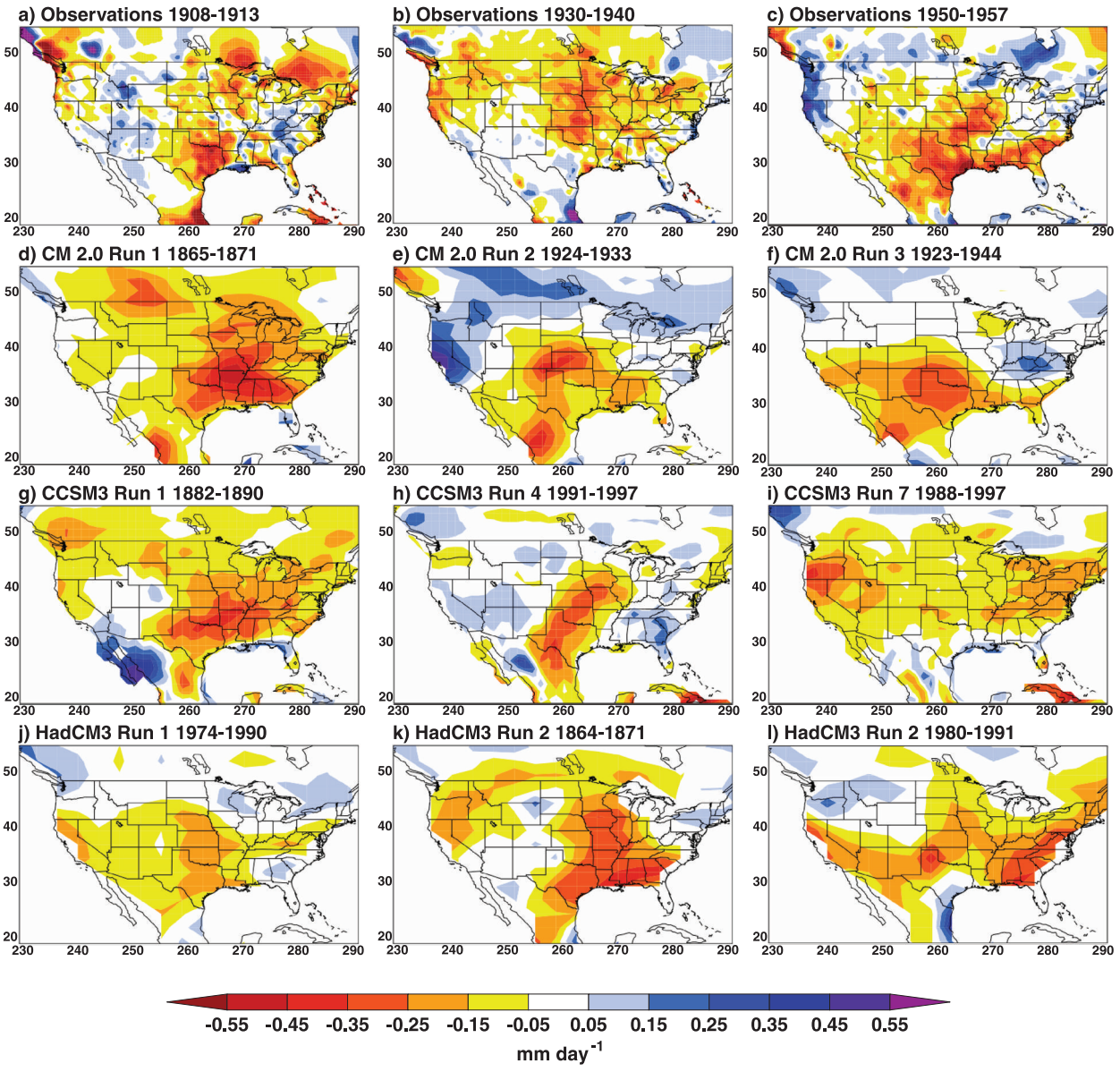

FIG. 3. Composite low-pass-filtered precipitation anomalies (mm day^{-1}) for a selection of the long-term drought periods identified in Table 5. Results are from (a)–(c) the observations, (d)–(f) CM2.0, (g)–(i) CCSM3, and (j)–(l) HadCM3.

America, as in the 1930s drought (Figs. 3g,l). In other cases, drought is restricted to only the Great Plains region, as was observed during the 1910s (Figs. 3h,k). For spatial patterns of the simulated droughts not shown in Fig. 3, see McCrary (2008).

By using a low-pass filter to identify long-term drought periods, we see that the models do simulate long-term drought conditions over the Great Plains that are comparable in severity, duration, and spatial extent as was observed. The next question to ask is if the simulated droughts are occurring for the same reasons as have been found in the observations. In the next section, we investigate the relative roles that tropical Pacific SST variability, tropical North Atlantic SST variability, and land–atmosphere interactions play in influencing Great Plains drought. One thing to keep in mind is that we are comparing the models against a sample of three observed droughts. Given the small observational sample size, it is difficult to make any definitive statements about the causes of these droughts; however, the mechanisms analyzed in the next section have been supported by results from idealized modeling experiments (Schubert et al. 2004a,b, 2009). Also, because CCSM3 has a larger ensemble size, it can in some ways be considered to be

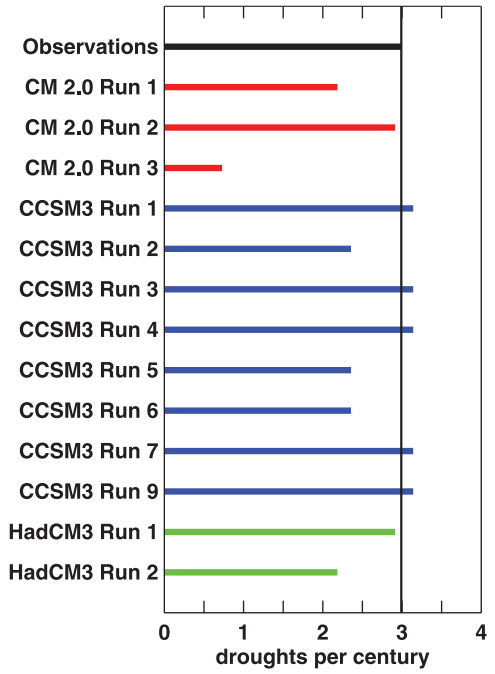

FIG. 4. The number of long-term droughts per century found using the low-pass-filtered Great Plains precipitation time series to identify long-term drought periods: observations (black), CM2.0 (red), CCSM3 (blue), and HadCM3 (green).

at an advantage over the other models. This is because there is a larger sample of simulated droughts with which to examine potential mechanism and more simulations to assess decadal variability in the model.

5. Processes that influence long-term drought

a. Low-frequency SST variability

As mentioned in the introduction, observational and modeling studies have implicated low-frequency variations in tropical Pacific and tropical North Atlantic SSTs as key features in the climate system that influence Great Plains precipitation variability on decadal time scales. Here, we compare SST patterns from the observed droughts with SST conditions found during the simulated droughts. In the following discussion, all SST and precipitation fields have been low-pass filtered to highlight variations that exist on time scales of 6 yr or longer. Also, the linear trend has been removed from all SST time series to account for the warming signal found in most of the world's oceans.

1) TROPICAL PACIFIC SSTS

Figure 5 shows the composite SST anomalies averaged over the peak drought period from a selection of the observed and simulated droughts. To summarize the SST conditions in the tropical Pacific from all of the observed and modeled droughts (identified in Table 5), Fig. 6a shows values for the composite SST anomalies from each drought period averaged over the Niño-3.4 region (5°S–5°N, 120°–170°W).

The composite maps show that SST patterns during the three observed drought periods were quite varied; however, common to all three of the droughts were cool conditions in the tropical Pacific (Figs. 5a–c, 6). The magnitude of the SST anomaly was largest during the 1950s and weakest during the 1930s (Fig. 6a). It has been argued by some that aerosol loading of the atmosphere due to the dust storms associated with the 1930s drought, may have played an important role in influencing the strength and position of this drought (Cook et al. 2008).

Global SST patterns also vary among the different simulated droughts (Figs. 5d–l). In agreement with the observations, the droughts simulated by HadCM3 are also associated with cool, La Niña–like conditions in the tropical Pacific. The SST anomalies from this model vary from case to case but tend to be quite large. In some cases, the maximum SST anomaly is not centered about the equator, as seen in the observations, but is displaced slightly to the south (Figs. 5k,l). The dynamical importance of the position of the SST anomaly in the tropical Pacific and its relationship with Great Plains precipitation has not been established.

The long-term droughts simulated by CM2.0 are also found to generally correspond with cooler than normal conditions in the tropical Pacific. In this model, all but two of the simulated long-term drought periods are associated with cool La Niña–like conditions in the Pacific; in some cases, these anomalies are large (Fig. 5f). The SST patterns associated with the CM2.0 run 3 1923–44 drought are strikingly similar to the composite global SST conditions found during the observed 1950s drought. Looking back at the precipitation anomalies associated with these two droughts (Figs. 3c,f), we see that the spatial coverage of dry conditions over the United States is also quite similar between these droughts.

In CCSM3, the relationship between Pacific SSTs and drought is somewhat less clear. Although a number of droughts simulated with this model do correspond with cooler than normal conditions in the Pacific, some of the more severe, long-lasting droughts are actually found to correspond with warmer than normal conditions in the tropical Pacific (CCSM3 run 1, 1882–90, and CCSM3 run 9, 1876–88). It is possible that the atmospheric response to SST variability and the associated teleconnection patterns are not well represented in CCSM3 (Joseph and Nigam 2006).

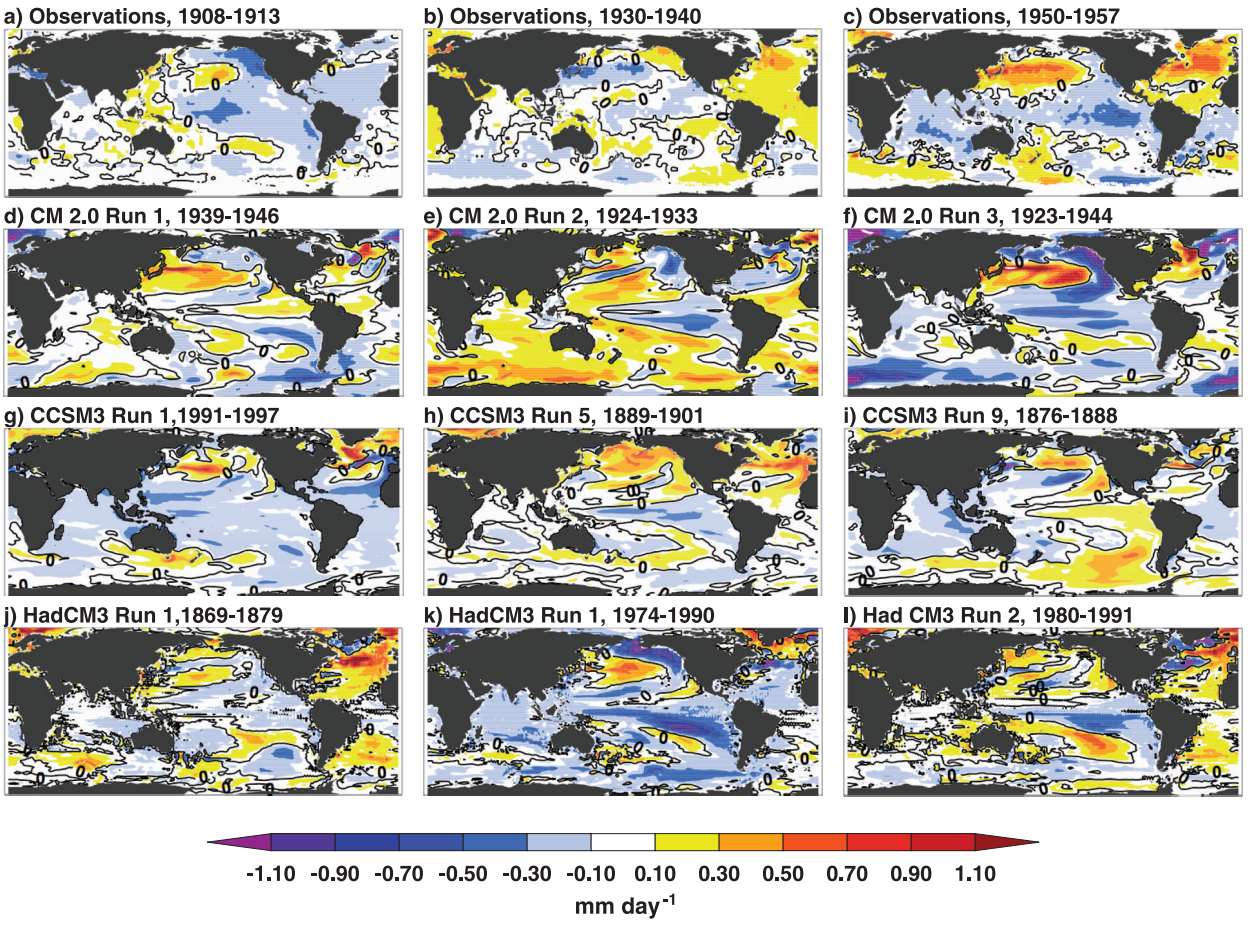

FIG. 5. Composite SST anomalies associated with the peak drought periods from a selection of the long-term droughts identified in Table 5. SST (°C) fields have been low-pass filtered and linearly detrended to remove the warming trend found in most ocean basins. Results are from (a)–(c) the observations, (d)–(f) CM2.0, (g)–(i) CCSM3, and (j)–(l) HadCM3.

2) TROPICAL NORTH ATLANTIC SSTS

Figure 6b shows values for the composite SST anomalies averaged over the tropical North Atlantic region (all Atlantic Ocean points from equator to 30°N) from the peak drought periods identified in Table 5. Although both the 1930s and 1950s observed droughts corresponded with warmer than normal conditions in the tropical North Atlantic region, the 1910s drought, on the other hand, was characterized by cooler than normal conditions in the tropical North Atlantic. The 1910s drought was weaker in both magnitude and spatial extent than either the 1930s or 1950s droughts, which could be partly due to the anomalously cool conditions found in the tropical North Atlantic during this time period.

In all three models, there is little if any systematic relationship between tropical Atlantic SST conditions and drought. About 50% of all of the droughts simulated with the models are found to correspond with warmer than normal conditions in the Atlantic region, whereas 50% correspond with cooler than normal conditions. Also, tropical Pacific and tropical Atlantic SSTs tend to be in phase with each other during the simulated drought periods, rather than out of phase, as found in the 1930s and 1950s observed droughts. Interestingly, in HadCM3, the droughts that correspond with warmer than normal conditions in the tropical North Atlantic tend to be the most severe droughts to occur in this model. This is similar to what has been found for the 1930s and 1950s droughts.

3) REGRESSION ANALYSIS

The relationship between Great Plains precipitation and global SST patterns can be further examined by using regression analysis. In Fig. 7 global SST anomalies have been regressed onto the Great Plains precipitation time series for the observations (Fig. 7a) and one integration from each model (Figs. 7b–d). In the figure, relationships that are statistically significant at the 95% confidence level are delineated by the black curve. We

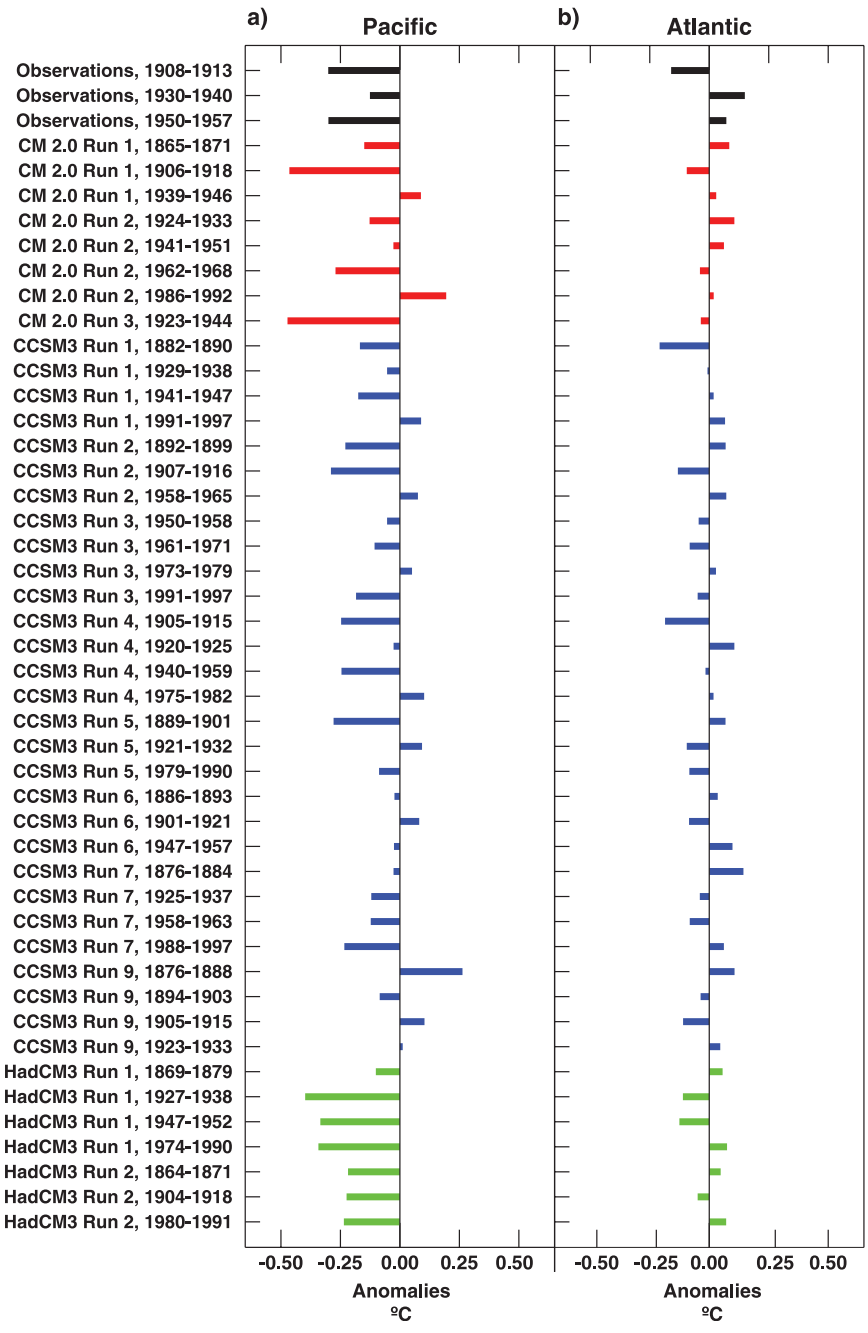

FIG. 6. Composite SST (°C) anomalies for the peak drought periods from the observed and simulated long-term droughts identified in Table 5 averaged over (a) the Niño-3.4 region and (b) the tropical North Atlantic region.

use the methods outlined by Bretherton et al. (1999) to determine the effective sample size of each population. Table 6 summarizes the linear relationships among tropical Pacific SSTs, tropical North Atlantic SSTs, and Great Plains precipitation. In this table, the tropical Pacific SST index and the tropical North Atlantic SST index have been correlated with the Great Plains precipitation time series. Correlations with an absolute value larger than 0.22 are statistically significant at the 95% confidence level.

In the observations, there is a positive and statistically significant relationship between Great Plains precipitation and tropical Pacific SSTs. This indicates that cooler than normal conditions in the tropical Pacific are associated with dry conditions over the Great Plains. Positive

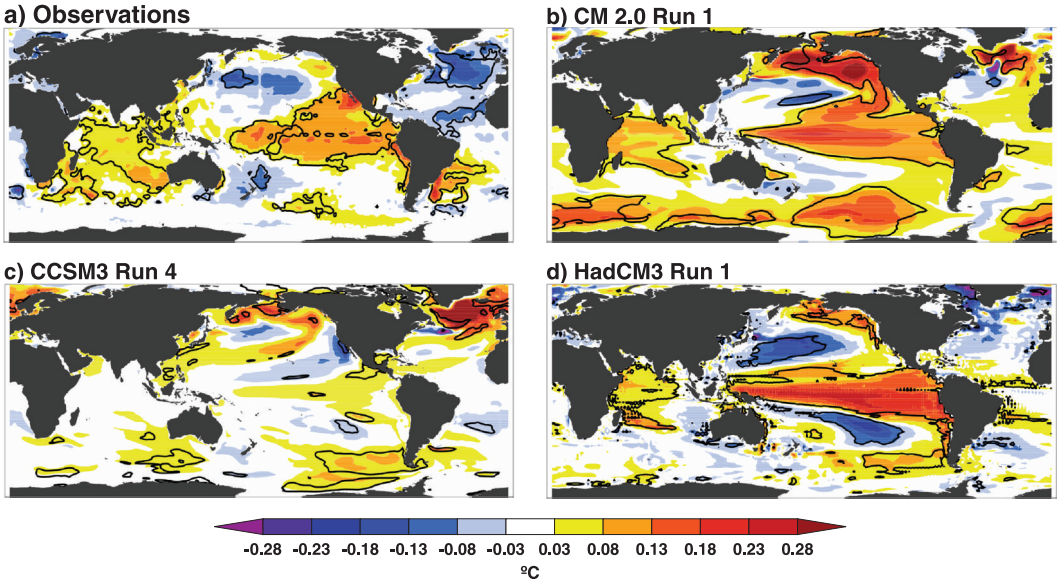

FIG. 7. Global SST anomalies [°C (std dev)$^{-1}$] regressed onto the Great Plains precipitation time series from (a) the observations and one run from each of the three models: (b) CM2.0, (c) CCSM3, and (d) and HadCM3. A low-pass filter has been applied to the precipitation and SST datasets to highlight relationships that exist on time scales of 6 yr or longer. The SST datasets have been linearly detrended to remove the impacts of global warming. Relationships that are significant at the 95% confidence level (95% CL) are delineated by the black curve.

relationships are also found in the Indian Ocean and on the eastern side of South America. Negative relationships are found in the North Pacific, North Atlantic, and the equatorial Atlantic region (Fig. 7). A negative relationship between tropical Atlantic SSTs and Great Plains precipitation indicates that warm conditions in the tropical Atlantic are associated with dry conditions over the Great Plains. As described in other studies, low-frequency variations in tropical Pacific SSTs and tropical North Atlantic SSTs have opposing influence on Great Plains precipitation (Table 6).

In both CM2.0 and HadCM3, the positive relationship between Great Plains precipitation and tropical Pacific SSTs is larger than what was observed. In CCSM3, on the other hand, the relationship with the tropical Pacific SSTs tends to be small and is generally not statistically significant. This supports the findings from the previous section that cooler than normal conditions can be expected to be found during long-term drought periods in CM2.0 and HadCM3 but the relationship in CCSM3 is less systematic. As for the tropical North Atlantic, correlations tend to be weak and are not statistically significant for almost all of the simulations. In all but three of the model integration (CM2.0 run 2, CCSM3 run 7, and CCSM3 run 9), Great Plains precipitation is positively correlated with low-frequency variations in the tropical North Atlantic. This also supports the findings from the previous section that, during the long-term drought periods, SSTs in the tropical Pacific and tropical North Atlantic tend to be of the same sign in the models. Further analysis is still needed to fully understand why the tropical Pacific and tropical North Atlantic vary in phase with each other in the models rather than out of phase with each other, as seen in the observations.

We can also look at the spatial relationship between tropical Pacific SSTs and North American precipitation. In Fig. 8, North American precipitation has been regressed onto the tropical Pacific SST index. In the observations, tropical Pacific SSTs primarily influence the southern portion of the Great Plains, with the largest positive relationships existing over the Gulf Coast region (Fig. 8a). Tropical Pacific SSTs also appear to be negatively correlated with precipitation over much of the southeastern United States. As for the three models, in both CM2.0 and HadCM3 tropical Pacific SSTs also primarily influence the southern Great Plains with large positive relationships occurring the Gulf Coast region (Figs. 8b,d). In both of these models, the positive relationship extends farther east into the South than is seen in the observations. In CCSM3, a positive relationship exists between tropical Pacific SSTs and precipitation over much of the United States, but this relationship is weak and generally not statistically significant (Fig. 8c). Also, the influence of tropical Pacific SST variability on precipitation in the southern Great Plains tends to be

TABLE 6. Correlation coefficients for the correlations between low-pass-filtered tropical Pacific SST anomalies (averaged over the Niño-3.4 region) and low-pass-filtered Great Plains precipitation and for the correlations between low-pass-filtered tropical North Atlantic SSTs (averaged between the equator and 30°N) and low-pass-filtered Great Plains precipitation. Correlations with absolute values larger than 0.22 are statistically significant at the 95% CL.

Dataset		Pacific	Atlantic
Observations		0.395	−0.254
CM2.0	Run 1	0.572	0.177
	Run 2	0.262	−0.233
	Run 3	0.531	0.027
CCSM3	Run 1	0.171	0.245
	Run 2	0.171	0.089
	Run 3	0.257	0.231
	Run 4	0.257	0.068
	Run 5	0.376	0.014
	Run 6	0.242	0.082
	Run 7	0.228	−0.083
	Run 9	0.216	−0.108
HadCM3	Run 1	0.569	0.102
	Run 2	0.643	0.082

weak. It appears that the tropical Pacific teleconnection patterns that influence North American hydroclimate are overestimated in CM2.0 and HadCM3 but underestimated in CCSM3. This is similar to the results found in Joseph and Nigam (2006).

b. *Land–atmosphere interactions*

As discussed in the introduction, cooler than normal SSTs in the tropical Pacific have been shown to primarily influence Great Plains precipitation during the cold season (October–March). As seen in section 3, most of the annual precipitation falls over the Great Plains during the warm season. It has been hypothesized by some that land–atmosphere interactions could act as a bridging mechanism between winter precipitation and summer precipitation. Up until this point, we have been investigating how low-frequency variations in the climate system may influence long-term drought over the Great Plains. Land–atmosphere interactions work on shorter (daily, weekly, monthly) time scales than SST variations. Although there is some evidence that deep soil moisture memory may add to the long-term persistence of drought conditions, in this section we are looking to see if land atmosphere interactions are active on monthly to seasonal time scales.

To investigate the relationship that exists between the land surface and the atmosphere, we look for linear relationships among precipitation, evapotranspiration, and soil moisture over the Great Plains. Because evapotranspiration is a key mechanism through which the land surface influences the atmosphere, we expect the coupling between the land surface and the atmosphere to be strongest during the wet season months (April–September). Scatterplots of monthly-mean anomalies of Great Plains precipitation, evapotranspiration, and soil moisture are shown in Fig. 9. Both the regression and correlation coefficients for each plot are shown on the figure and denoted by ''a'' and ''r,'' respectively. Also, all correlations shown in the figure are statistically significant at the 95% confidence level based on a two-tailed *t* test.

In VIC, there exists a positive relationship between precipitation, evapotranspiration, and soil moisture. The relationship among these variables is similar in CM2.0, but it is stronger than observed in CCSM3 and weaker than observed in HadCM3. In CCSM3, the slope of the least squares fit line between precipitation and evapotranspiration is almost 3 times larger than in VIC. Also, the scatter about the line is very small, which is one indication that the linear fit does a good job representing this relationship in this model. One possible explanation for the tight coupling between these two variables is that much of the precipitation that reaches the surface is immediately reevaporated into the atmosphere, never having a chance to become part of the soil moisture. Previous studies have shown that the Community Atmosphere Model (CAM), the atmospheric component of CCSM3, tends to overestimate light to moderate rainfall and underestimate heavy or convective rainfall (Sun et al. 2006). This light to moderate rainfall is easily intercepted by the vegetation at the surface and tends to be immediately reevaporated into the atmosphere (DeMott et al. 2007). Immediate reevaporation of precipitation from the surface could also partially explain why large changes in precipitation account for only small changes in soil moisture and why large changes in evapotranspiration are also associated with only small changes in soil moisture. It is possible that strong land–atmosphere coupling in CCSM3 causes precipitation rates over the Great Plains to respond too strongly to small changes in surface conditions, thereby promoting drought conditions.

In HadCM3, on the other hand, the linear relationship between precipitation and evapotranspiration is only about half as strong as in VIC and one-fifth as strong as the relationship found in CCSM3. Also, precipitation accounts for only 6% of the variance in evapotranspiration in HadCM3 (i.e., there is significant scatter about the least squares fit line). The relationship between soil moisture and evapotranspiration is similarly weak in HadCM3. This points to a lack of interaction between the land surface and the atmosphere in this model. This conclusion is not unique to this study; the Global Land–Atmosphere Coupling Experiment (GLACE) also found that the land surface and atmosphere to be decoupled in

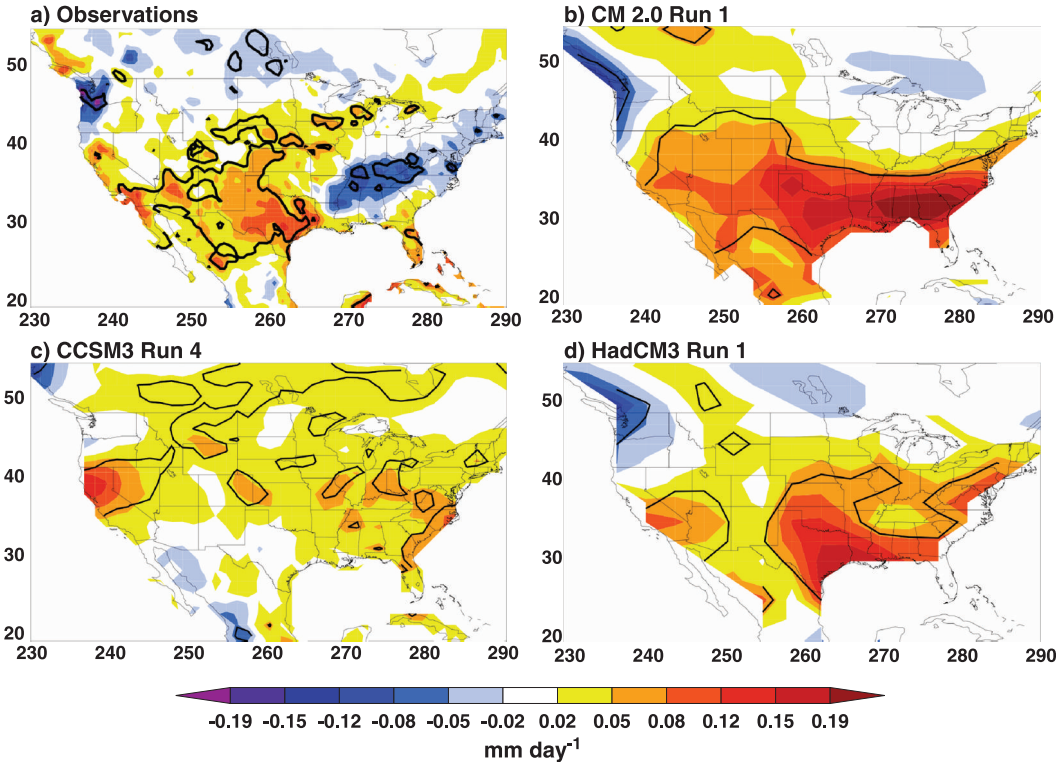

FIG. 8. North American precipitation anomalies [mm day^{-1} (std dev)$^{-1}$] regressed onto the index of tropical Pacific SSTs from (a) the observations and one run from each of the three models: (b) CM2.0, (c) CCSM3, and (d) HadCM3. A low-pass filter has been applied to the precipitation and SST datasets to highlight relationships that exist on time scales of 6 yr or longer. The SST time series has been linearly detrended to remove the impacts of global warming. Relationships that are significant at the 95% CL are delineated by the black curve.

HadCM3 (Koster et al. 2004, 2006). Lawrence and Slingo (2005) have studied the land surface of HadCM3 in detail and argue that the weak soil moisture–precipitation feedback in HadAM3 (the atmospheric component of HadCM3) is related to one of two factors, either how the boundary layer adjusts to changes in surface forcing (i.e., how the boundary layer adjusts to changes in latent and sensible heat fluxes) or how moist convection responds to boundary layer conditions (i.e., the relationship between the stability of the boundary layer and the timing and initiation of moist convection). Whatever the cause, the lack of coupling between the land surface and the atmosphere indicates that land–atmosphere interactions do not play a strong role in influencing Great Plains drought in this model.

Land–atmosphere coupling in CM2.0 is similar to what is seen from VIC. Precipitation, evapotranspiration, and soil moisture all exhibit positive linear relationships, and local evapotranspiration is clearly linked to precipitation. This suggests that the importance of land–atmosphere interactions in the magnitude and persistence of long-term drought over the Great Plains is similar in CM2.0 as compared with VIC.

6. Concluding remarks

The present study has sought to evaluate the ability of three CGCMs used in the AR4 to simulate long-term drought over the Great Plains region of the United States. Our goal has been to determine whether the models are credible for use in future drought assessment studies. Assessing the credibility of these models has required examining their ability to represent 1) the climatology of the hydrologic cycle of the Great Plains; 2) the variability of Great Plains precipitation, including the frequency of occurrence of long-term droughts; and 3) the physical processes that correspond with long-term droughts.

Reproducing the climatology of the hydrologic cycle over the Great Plains proved to be a challenge for the models. Although the broad features of the annual cycle are captured by the models (e.g., the Great Plains are wet during the warm season and dry during the cold season), they all experience some problems representing either the timing or the amplitude of the seasonal cycles of precipitation, evapotranspiration, and soil moisture. Both CM2.0 and HadCM3 overestimate the amplitude of the seasonal cycles of precipitation and evapotranspiration;

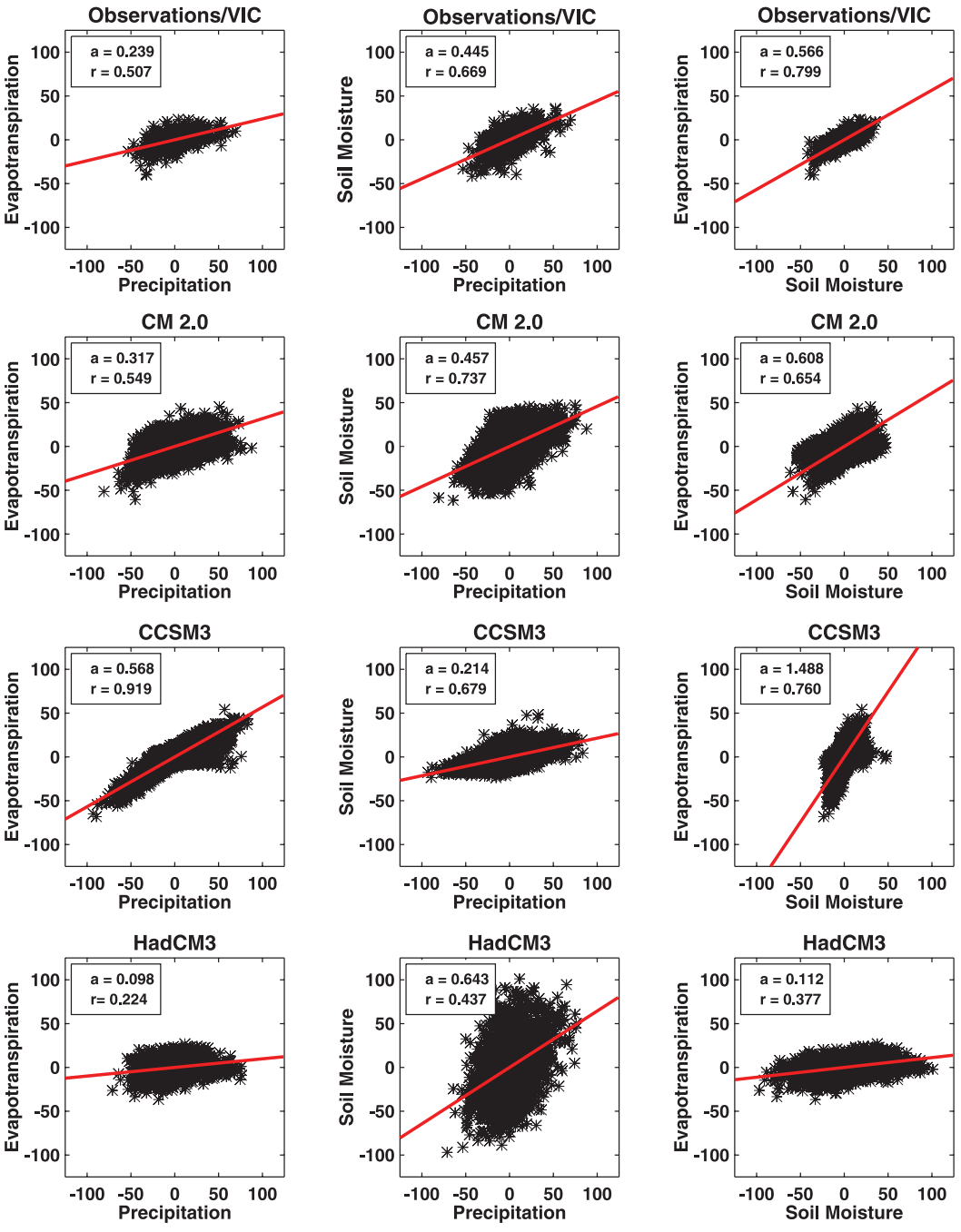

FIG. 9. Scatterplots of monthly-mean anomalies (mm month^{-1}) for the Great Plains region for (left) precipitation vs evapotranspiration, (middle) precipitation vs soil moisture, and (right) soil moisture vs evapotranspiration. Values shown are only from the wet season months (April–September), when land–atmosphere interactions are known to be active.

however, in CCSM3, both precipitation and evapotranspiration experience large, unrealistic decreases between the months of June and August. The impact that this seasonal drought has on long-term drought has yet to be investigated for CCSM3, but it is likely that this feature influences the coupling between land surface and the atmosphere. We also show that the treatment of total column soil moisture varies among the models, possibly due to differences in the depth of the soil column being considered; differences in the hydraulic properties of the

soils, including texture and porosity; and differences in the root depths of the vegetation in the Great Plains regions. These parameters are prescribed as input to the models and were difficult to analyze based on the data available.

By applying a low-pass filter to the Great Plains precipitation time series, we identified a number of long-term drought periods in the observed and simulated twentieth centuries. The models appear to capture the observed frequency of long-term droughts, with two to three long-term droughts occurring per century in most simulations, as compared to the three droughts found in the observed time record. The simulated and observed droughts are also found to be comparable in duration, severity, and spatial extent.

The mechanisms that potentially cause these long-term droughts in the simulations are found to vary between the models. Previous studies have indicated that, during the observed twentieth century, cool La Niña–like conditions in the tropical Pacific, warmer than normal conditions in the tropical North Atlantic, and land–atmosphere feedbacks all play key roles in the persistence of drought conditions over the Great Plains. In the models, however, these processes have been shown to influence Great Plains precipitation with differing degrees of importance.

In both CM2.0 and HadCM3, low-frequency variations in Great Plains precipitation are found to be correlated with low-frequency variations in tropical Pacific SSTs, although this relationship is somewhat overestimated by the models. Cool La Niña–like conditions in the tropical Pacific are also found to be associated with simulated droughts in both of these models. In CCSM3, on the other hand, there appears to be no systematic relationship between tropical Pacific SSTs and Great Plains precipitation. A number of severe droughts simulated by this model were found to correspond with warmer than normal conditions in the tropical Pacific. It appears that the atmosphere in CCSM3 does not respond as strongly to fluctuations in tropical Pacific SSTs as the atmosphere does in the other CGCMs or in the observations. More recent versions of the NCAR CCSM have been shown to better simulate tropical Pacific SST variability, which may improve the connection between the tropics and Great Plains precipitation (Gent et al. 2010).

The present study has also shown that there is little if any systematic relationship between low-frequency variations in tropical North Atlantic SSTs and Great Plains precipitation in the models. Although there is some evidence to suggest that warmer than normal conditions in the tropical North Atlantic may enhance drought conditions over the Great Plains region in HadCM3, idealized studies forced with SSTs that emphasize variations in the tropical North Atlantic might be better suited to look at the specific role that this region plays in influencing precipitation variability over the Great Plains (see Schubert et al. 2009).

In both the observations and the CGCMs, SST variability accounts for only a small fraction (at most 30%) of the variance in Great Plains precipitation. Other processes such as internal atmospheric variability and land–atmosphere interactions most likely play important roles in the generation of Great Plains drought. The degree to which land–atmosphere interactions potentially influence Great Plains drought varies among the models. In CCSM3, for example, although there appears to be little if any systematic relationship between Great Plains precipitation and tropical Pacific SSTs, the land surface and the atmosphere are found to be tightly coupled in this model and local feedbacks may help to trigger drought conditions. In HadCM3, the land surface and the atmosphere are found to be only weakly coupled, indicating that land–atmosphere feedbacks may not play a significant role in the persistence of drought conditions over the Great Plains in this model. It is more likely that external forcing from the tropical Pacific and internal atmospheric variability cause long-term droughts in this model.

Unfortunately, with fully coupled simulations it is impossible to separate the effects of SST forcing and land–atmosphere interactions. One way to investigate the degree to which land–atmosphere interactions influence long-term drought might be to perform idealized SST experiments where global SSTs are set to the seasonally varying climatology. In these experiments, precipitation will only be influenced by internal atmospheric variability and land–atmosphere feedbacks, thus allowing us to see if long-term drought periods occur in these models without low-frequency variations in SSTs.

Based on the findings from this study, of the three models, CM2.0 best captures the observed climatology of the Great Plains region and the mechanisms known to be associated with long-term drought conditions. Both CCSM3 and HadCM3 have difficulty representing the climatology of the Great Plains region as well as the key features in the climate system that have been shown to be associated with drought. For this reason, we argue that CM2.0 would be best suited for use in future drought assessment studies. However, although CM2.0 does appear to capture the observed variability in twentieth-century Great Plains drought, this does not guarantee that CM2.0 will capture the future behavior of drought over the Great Plains region in a warming climate. Until these models better represent the relationship between low-frequency variations in tropical Pacific SSTs and Great Plains precipitation and local land–atmosphere

interactions are better simulated, future drought assessment studies involving these models should be treated with caution.

Acknowledgments. This work was supported by the National Science and Technology Center for Multi-Scale Modeling of Atmospheric Processes, managed by Colorado State University under Cooperative Agreement ATM-0425247. The authors would like to acknowledge the modeling groups, the Program for Climate Model Diagnosis and Intercomparison (PCMDI) and the WCRP's Working Group on Coupled Modelling (WGCM), for their roles in making available the WCRP CMIP3 multimodel dataset. Support of this dataset is provided by the Office of Science, U.S. Department of Energy. The authors would also like to thank Kostas Andreadis at the University of Washington for providing the historical hydrologic model dataset used in this research.

REFERENCES

Andreadis, K. M., E. A. Clark, A. W. Wood, A. F. Hamlet, and D. P. Lettenmaier, 2005: Twentieth-century drought in the conterminous United States. *J. Hydrometeor.,* **6,** 985–1001.

Borchert, J. R., 1950: The climate of the central North American grassland. *Ann. Assoc. Amer. Geogr.,* **40,** 1–39.

——, 1971: Dust Bowl in 1970s. *Ann. Assoc. Am. Geogr.,* **61,** 1–22.

Bretherton, C. S., M. Widmann, V. P. Dymnikov, J. M. Wallace, and I. Bladé, 1999: The effective number of spatial degrees of freedom of a time-varying field. *J. Climate,* **12,** 1990–2009.

Cherkauer, K. A., and D. P. Lettenmaier, 2003: Simulation of spatial variability in snow and frozen soil. *J. Geophys. Res.,* **108,** 8858, doi:10.1029/2003JD003575.

Collins, W. D., and Coauthors, 2006: The Community Climate System Model Version 3 (CCSM3). *J. Climate,* **19,** 2122–2143.

Cook, B. I., R. L. Miller, and R. Seager, 2008: Dust and sea surface temperature forcing of the 1930s "Dust Bowl" drought. *Geophys. Res. Lett.,* **35,** L08710, doi:10.1029/2008GL033486.

Cook, E. R., R. Seager, M. A. Cane, and D. W. Stahle, 2007: North American drought: Reconstructions, causes, and consequences. *Earth Sci. Rev.,* **81** (1–2), 93–134.

Delworth, T. L., and Coauthors, 2006: GFDL's CM2 global coupled climate models. Part I: Formulation and simulation characteristics. *J. Climate,* **19,** 643–674.

DeMott, C. A., D. A. Randall, and M. Khairoutdinov, 2007: Convective precipitation variability as a tool for general circulation model analysis. *J. Climate,* **20,** 91–112.

Eltahir, E. A. B., 1998: A soil moisture–rainfall feedback mechanism 1. Theory and observations. *Water Resour. Res.,* **34,** 765–776.

Findell, K. L., and E. A. B. Eltahir, 1997: An analysis of the soil moisture-rainfall feedback, based on direct observations from Illinois. *Water Resour. Res.,* **33,** 725–735.

Gent, P. R., S. G. Yeager, R. B. Neale, S. Levis, and D. A. Baily, 2010: Improvements in a half degree atmosphere/land version of CCSM. *Climate Dyn.,* doi:10.1007/s00382-009-0614-8, in press.

Gordon, C., C. Cooper, C. Senior, H. Banks, J. Gregory, T. Johns, J. Mitchell, and R. Wood, 2000: The simulation of SST, sea ice extents and ocean heat transports in a version of the Hadley Centre coupled model without flux adjustments. *Climate Dyn.,* **16** (2–3), 147–168.

Guo, Z., and Coauthors, 2006: GLACE: The Global Land–Atmosphere Coupling Experiment. Part II: Analysis. *J. Hydrometeor.,* **7,** 611–625.

Herweijer, C., R. Seager, and E. Cook, 2006: North American droughts of the mid to late nineteenth century: A history, simulation and implication for Mediaeval drought. *Holocene,* **16,** 159–171, doi:10.1191/0959683606hl917rp.

Jacobs, K., D. B. Adams, and P. Gleick, 2000: Potential consequences of climate variability and change for the water resources of the United States. *U.S. National Assessment of the Potential Consequences of Climate Variability and Change,* Cambridge University Press, 405–435.

Joseph, R., and S. Nigam, 2006: ENSO evolution and teleconnections in IPCC's twentieth-century climate simulations: Realistic representation? *J. Climate,* **19,** 4360–4377.

Kallis, G., 2008: Droughts. *Ann. Rev. Environ. Res.,* **33,** 85–118, doi:10.1146/annurev.environ.33.081307.123117.

Kalnay, E., and Coauthors, 1996: The NCEP/NCAR 40-Year Reanalysis Project. *Bull. Amer. Meteor. Soc.,* **77,** 437–471.

Koster, R. D., M. J. Suarez, and M. Heiser, 2000: Variance and predictability of precipitation at seasonal-to-interannual timescales. *J. Hydrometeor.,* **1,** 26–46.

——, ——, R. W. Higgins, and H. M. Van den Dool, 2003: Observational evidence that soil moisture variations affect precipitation. *Geophys. Res. Lett.,* **30,** 1241, doi:10.1029/2002GL016571.

——, and Coauthors, 2004: Regions of strong coupling between soil moisture and precipitation. *Science,* **305,** 1138–1140.

——, and Coauthors, 2006: GLACE: The Global Land–Atmosphere Coupling Experiment. Part I: Overview. *J. Hydrometeor.,* **7,** 590–610.

Lawrence, D. M., and J. M. Slingo, 2005: Weak land–atmosphere coupling strength in HadAM3: The role of soil moisture variability. *J. Hydrometeor.,* **6,** 670–680.

Liang, X., D. P. Lettenmaier, E. F. Wood, and S. J. Burges, 1994: A simple hydrologically based model of land surface water and energy fluxes for general circulation models. *J. Geophys. Res.,* **99,** 14 415–14 428.

——, ——, and ——, 1996: One-dimensional statistical dynamic representation of subgrid spatial variability of precipitation in the two-layer variable infiltration capacity model. *J. Geophys. Res.,* **101,** 21 403–21 422.

Livezey, R. E., and T. M. Smith, 1999: Covariability of aspects of North American climate with global sea surface temperatures on interannual to interdecadal timescales. *J. Climate,* **12,** 289–302.

McCabe, G. J., J. L. Betancourt, S. T. Gray, M. A. Palecki, and H. G. Hidalgo, 2008: Associations of multi-decadal sea-surface temperature variability with US drought. *Quat. Int.,* **188,** 31–40, doi:10.1016/j.quaint.2007.07.001.

McCrary, R. R., 2008: Great Plains drought in simulations of the twentieth century. M.S. thesis, Department of Atmospheric Science, Colorado State University, 199 pp.

McKee, T. B., N. J. Doesken, and J. Kleist, 1993: The relationship of drought frequency and duration to time scales. *Proc. Eighth Conf. on Applied Climatology,* Boston, MA, Amer. Meteor. Soc., 179–184.

Meehl, G. A., C. Covey, T. Delworth, M. Latif, B. McAvaney, J. F. B. Mitchell, R. J. Stouffer, and K. E. Taylor, 2007: The WCRP CMIP3 multimodel dataset: A new era in climate change research. *Bull. Amer. Meteor. Soc.,* **88,** 1383–1394.

Mitchell, T., and P. Jones, 2005: An improved method of constructing a database of monthly climate observations and associated high-resolution grids. *Int. J. Climatol.,* **25,** 693–712, doi:10.1002/joc.1181.

Namias, J., 1960: Factors in the initiation, perpetuation and termination of drought. IASH Commission of Surface Waters Publication 51, 81–94.

——, 1983: Some causes of United States drought. *J. Climate Appl. Meteor.,* **22,** 30–39.

——, 1991: Spring and summer 1988 drought over the contiguous United States—Causes and prediction. *J. Climate,* **4,** 54–65.

Oglesby, R. J., 1991: Springtime soil moisture, natural climatic variability, and North American drought as simulated by the NCAR Community Climate Model 1. *J. Climate,* **4,** 890–897.

——, and D. J. Erickson, 1989: Soil moisture and the persistence of North American drought. *J. Climate,* **2,** 1362–1380.

Pal, J. S., and E. A. B. Eltahir, 2001: Pathways relating soil moisture conditions to future summer rainfall within a model of the land–atmosphere system. *J. Climate,* **14,** 1227–1242.

Rayner, N. A., D. E. Parker, E. B. Horton, C. K. Folland, L. V. Alexander, D. P. Rowell, E. C. Kent, and A. Kaplan, 2003: Global analyses of sea surface temperature, sea ice, and night marine air temperature since the late nineteenth century. *J. Geophys. Res.,* **108,** 4407, doi:10.1029/2002JD002670.

Robock, A., K. Y. Vinnikov, G. Srinivasan, J. K. Entin, S. E. Hollinger, N. A. Speranskaya, S. Liu, and A. Namkhai, 2000: The Global Soil Moisture Data Bank. *Bull. Amer. Meteor. Soc.,* **81,** 1281–1299.

Ropelewski, C. F., and M. S. Halpert, 1986: North American precipitation and temperature patterns associated with the El Niño/Southern Oscillation (ENSO). *Mon. Wea. Rev.,* **114,** 2352–2362.

Ruiz-Barradas, A., and S. Nigam, 2006: IPCC's twentieth-century climate simulations: Varied representations of North American hydroclimate variability. *J. Climate,* **19,** 4041–4058.

Schubert, S. D., M. J. Suarez, P. J. Pegion, R. D. Koster, and J. T. Bacmeister, 2004a: Causes of long-term drought in the U.S. Great Plains. *J. Climate,* **17,** 485–503.

——, ——, ——, ——, and ——, 2004b: On the cause of the 1930s Dust Bowl. *Science,* **303,** 1855–1859.

——, ——, ——, ——, and ——, 2008: Potential predictability of long-term drought and pluvial conditions in the U.S. Great Plains. *J. Climate,* **21,** 802–816.

——, and Coauthors, 2009: A U.S. CLIVAR project to assess and compare the responses of global climate models to drought-related SST forcing patterns: Overview and results. *J. Climate,* **22,** 5251–5272.

Seager, R., N. Harnik, W. A. Robinson, Y. Kushnir, M. Ting, H.-P. Huang, and J. Velez, 2005a: Mechanisms of ENSO-forcing of hemispherically symmetric precipitation variability. *Quart. J. Roy. Meteor. Soc.,* **131B,** 1501–1527, doi:10.1256/qj.04.96.

——, Y. Kushnir, C. Herweijer, N. Naik, and J. Velez, 2005b: Modeling of tropical forcing of persistent droughts and pluvials over western North America: 1856–2000. *J. Climate,* **18,** 4065–4088.

——, and Coauthors, 2007: Model projections of an imminent transition to a more arid climate in southwestern North America. *Science,* **316,** 1181–1184, doi:10.1126/science.1139601.

——, Y. Kushnir, M. Ting, M. Cane, N. Naik, and J. Miller, 2008: Would advance knowledge of 1930s SSTs have allowed prediction of the Dust Bowl drought? *J. Climate,* **21,** 3261–3281.

Solomon, S., D. Qin, M. Manning, M. Marquis, K. Averyt, M. M. B. Tignor, H. L. Miller Jr., and Z. Chen, Eds., 2007: *Climate Change 2007: The Physical Science Basis*. Cambridge University Press, 996 pp.

Sun, Y., S. Solomon, A. Dai, and R. W. Portmann, 2006: How often does it rain? *J. Climate,* **19,** 916–934.

Sutton, R. T., and D. L. R. Hodson, 2005: Atlantic Ocean forcing of North American and European summer climate. *Science,* **309,** 115–118, doi:10.1126/science.1109496.

——, and ——, 2007: Climate response to basin-scale warming and cooling of the North Atlantic Ocean. *J. Climate,* **20,** 891–907.

Ting, M., and H. Wang, 1997: Summertime U.S. precipitation variability and its relation to Pacific sea surface temperature. *J. Climate,* **10,** 1853–1873.

Trenberth, K. E., and G. W. Branstator, 1992: Issues in establishing causes of the 1988 drought over North America. *J. Climate,* **5,** 159–172.

Woodhouse, C. A., and J. T. Overpeck, 1998: 2000 years of drought variability in the central United States. *Bull. Amer. Meteor. Soc.,* **79,** 2693–2714.

Zhang, Y., J. M. Wallace, and D. S. Battisti, 1997: ENSO-like interdecadal variability: 1900–93. *J. Climate,* **10,** 1004–1020.